



IMAGING OF ROD-AIRFOIL AEROACOUSTICS USING A LOW-COST ACOUSTIC CAMERA

M. Debrouwere, L. Uyttersprot, J. Verwilligen, S. Pröbsting,
D. G. Simons and F. Scarano
Faculty of Aerospace Engineering
Delft University of Technology
Kluyverweg 1, 2629 HS Delft

ABSTRACT

Along with stricter noise regulations in aviation comes the requirement to identify and eliminate sources of noise in aerodynamic designs. For this purpose, a phased array and data acquisition system (acoustic camera) was designed and built by students of the Faculty of Aerospace Engineering of Delft University of Technology. The performance of the phased array and different beamforming algorithms is evaluated with a variety of test cases, representative for the experiments conducted in moderate size wind tunnels (models of 10cm to 30cm, working distance of 1m to 2m) as typically available in university laboratories. The considered test cases are rod-airfoil combinations, which produce low-frequency tonal noise. The scaled models are tested in an open jet non-anechoic vertical wind tunnel at flow speeds ranging from 15ms^{-1} to 40ms^{-1} . The experiments present several challenges, namely the low level of the emitted noise, the required high spatial resolution and the refraction of sound waves travelling through the shear layer. The study discusses the specific developments and optimization of the low-cost acoustic camera for use in the non-anechoic open jet wind tunnel of moderate size.

1 Introduction

Along with stricter noise regulations in aviation comes the requirement to identify and eliminate noise in aerodynamic designs. For this purpose an acoustic array can be used as a diagnostic tool which maps the noise sources. Over the past ten years extensive research has been done to improve the functioning of those acoustic arrays [1], [4]. However, most acoustic cameras remain very expensive. As an answer to this matter a group students of the Faculty of Aerospace Engineering of the Delft University of Technology designed and built a phased array and data acquisition system at the fraction of the cost of current commercially available

technology.

Originally this acoustic array was designed with as main purpose the noise source identification of fly-overs of mid-range to long-range passenger aircraft. However, this paper aims to analyse the performance of the phased array when used for a different application, namely the application of the phased array for noise source identification in wind tunnel experiments. For this purpose a variety of test cases, representative for experiments conducted in moderate size wind tunnels (models of 10cm to 30cm, working distance 1 m to 2m) as typically available in university laboratories, were performed. The considered test cases are rod-airfoil combinations, which produce low frequency tonal noise. The scaled models are tested in an open jet non-anechoic vertical wind tunnel at flow speeds ranging from 15 ms^{-1} to 40 ms^{-1} . The wind tunnel environment differs from the original fly-over environment in a number of ways which present several challenges for the noise source mapping. Among those challenges are the low level of the emitted noise, the required high spatial resolution and the refraction of sound waves travelling through the shear layer. This study discusses the specific developments and optimization of the low-cost acoustic camera for use in the non-anechoic open jet wind tunnel of moderate size.

The second section will discuss the experimental set-up and procedures that were used to analyse the performance of the phased array. It will first give more details about the test case itself, namely the rod-airfoil combinations. Consequently a more detailed description of the used acoustic camera together with the implemented adaptations specific for the wind tunnel test case will be given. The third section will provide the results together with a discussion.

2 Experimental set-up and procedures

2.1 Description of test cases

The performance of the acoustic camera is evaluated with a variety of measurements performed in an open-jet non-anechoic vertical wind tunnel of the Delft University of Technology at flow speeds ranging from 15 ms^{-1} to 40 ms^{-1} . This wind tunnel has a circular cross-section of 60cm. The phased array was placed at a distance of 96.5cm from the centre line of the wind tunnel as visible in Fig. 1(a). It is important to note that the centre point of the phased array was placed 7cm to the left of the centre line of the wind tunnel. All test cases consist of a rod-airfoil combination, where the generic airfoil, which has a symmetric profile with a trailing edge thickness of 3 mm, is placed parallel to the phased array. Three different cases were used: one rod parallel to the airfoil (Fig. 1(a)), one rod perpendicular to the airfoil (Fig. 1(b)) and two rods perpendicular to the airfoil (Fig. 1(c)). Here, the rods are always placed at a distance of 18.5cm in front of the leading edge of the airfoil.

The rod-airfoil configuration in general is used as a benchmark test case for aeroacoustic assessments of vortex-structure interaction broadband noise [2] [3]. In this case the airfoil is embedded in the wake of the upstream rod. This can represent features of a high-lift device configuration or a landing gear. In the rod-airfoil test set-up one main source of noise emission is the vorticity shed by the rod convecting over the airfoil. Furthermore the blunt trailing edge

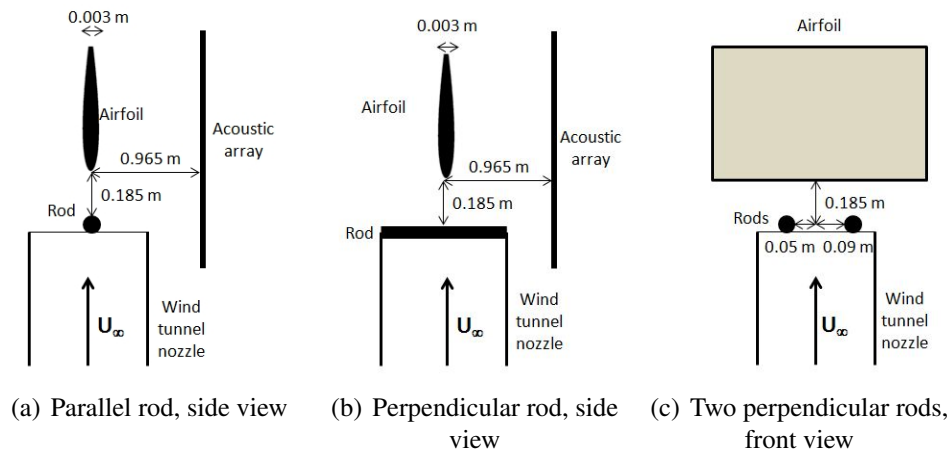


Figure 1: Schematic overview of the test set-up (not drawn up to scale)

of the airfoil and the associated vortex shedding also causes noise emission.

2.2 Acoustic camera for wind tunnel measurements

In order to identify noise sources in aerodynamic test cases a phased array and data acquisition system (acoustic camera), designed and built by a group of students of the Faculty of Aerospace Engineering of Delft University of Technology, was used. The acoustic camera consists of 32 microphone channels, placed on a flat plate of 2.38 m by 1.60 m in a spiral configuration. For all measurements the sampling frequency was set at 50 kHz. Furthermore the sampling time per block was 0.2 s, which corresponds to a frequency resolution of 5 Hz. Furthermore the sampling time per block was set to 0.2 s. For every block of 0.2 s a data transfer of 0.4 s is needed. This results in a total measurement time of 0.6 s times the number of blocks. The acoustic camera supports different beamforming algorithms. However, for clarity, only the conventional beamforming algorithm will be used in this paper. For a more detailed description of the acoustic camera the reader is referred to [8]. The next sections will describe modifications of the original beamforming software to tailor the acoustic camera to wind tunnel measurements.

Wind-correction

The key ingredient in almost any beamforming algorithm is the steering vector [5], shown in Eq. 1. It is a function of the frequency f , the distance from a microphone to the scan point $\|\mathbf{x}_m - \mathbf{x}_s\|$ and the travel time Δt , the time required for the sound to arrive at the microphone. When no wind is present, this travel time is a linear function of the distance to the scan point, since sound waves travel with the speed of sound. When a constant wind is present, this calculation is more comprehensive. For our particular experiment it was assumed that the wind exiting the tunnel has a uniform velocity while the air is stagnant outside this jet. The average flow velocity is

then used to compute the steering vector [5] given by

$$\mathbf{g} = \frac{-e^{-2\pi i f \Delta t (\mathbf{x}_m \cdot \mathbf{x}_s)}}{4\pi \|\mathbf{x}_m - \mathbf{x}_s\|} \quad (1)$$

If a point source at location \mathbf{x}_s is considered under zero wind conditions, the sound will move outward in a spherical fashion. If now a constant airspeed is introduced, each consecutive sphere will have moved with respect to the previous one with the speed of the flow. Therefore the source appears to be at a different place at each instant in time. The problem is now to find the time Δt at which the sound wave has reached the observer.

In Fig. 2 the problem as described above is depicted. Here $V\Delta t$ is the distance the ‘virtual’ source has moved when the sound arrives at the observer and x_v is the distance to the virtual source at that time. The angle α can be computed using the definition of the dot product (Eq. 2), elaborated in Eq. 3.

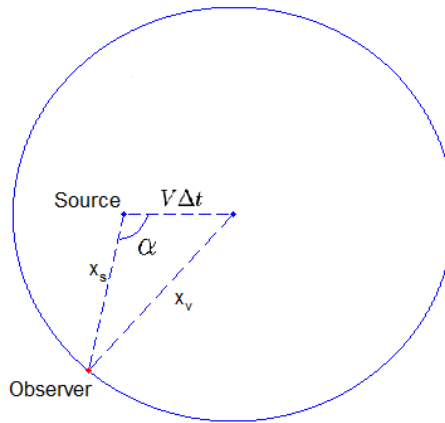


Figure 2: The situation after time Δt

$$\mathbf{x}_s \cdot \mathbf{V}\Delta t = \|\mathbf{x}_s\| \|\mathbf{V}\Delta t\| \cos \alpha \quad (2)$$

$$\alpha = \arccos \left(\frac{\mathbf{x}_s \cdot \mathbf{V}\Delta t}{\|\mathbf{x}_s\| \|\mathbf{V}\Delta t\|} \right) \quad (3)$$

With α known and observing that x_v is equal to the speed of sound c times the travel time, the law of cosines can be formulated (Eq. 4). This is a quadratic equation, so the quadratic formula can be used to determine Δt (Eq. 5).

$$x_v^2 = (c\Delta t)^2 = x_s^2 + (V\Delta t)^2 - x_s V\Delta t \cos \alpha \quad (4)$$

$$\Delta t = \frac{x_s V\Delta t \cos \alpha \pm \sqrt{(-x_s V\Delta t \cos \alpha)^2 - 4(V^2 - c^2)x_s^2}}{2(V^2 - c^2)} \quad (5)$$

The results with this corrected steering vector are satisfying. The effect can be seen in Fig. 3 and 4. The source is expected close to the white line of the rod. If no wind correction is applied on the steering vector the source is detected further downstream of the rod (Fig. 3). When the corrected steering vector is used the position of the source appears to be more accurate (Fig. 4). In this case the rod was parallel to the airfoil's leading edge and has a diameter of 4 mm. The wind speed is 30 m/s and the selected frequency range is 1550 to 1620 Hz, covering the expected shedding frequency based on Strouhal's relation.

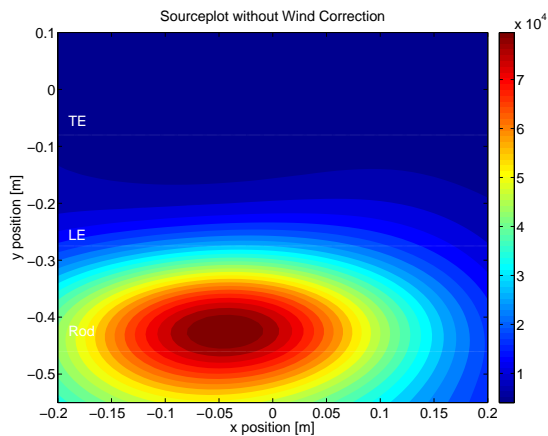


Figure 3: Without wind correction

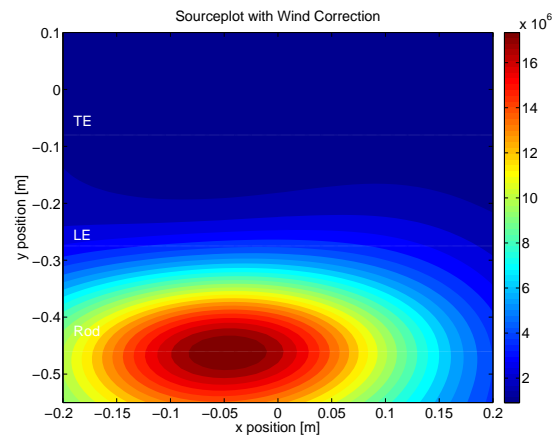


Figure 4: With wind correction

Averaging

In order to improve the results, multiple measurements were combined to filter out noise from the environment. The data acquisition system runs for several seconds during which multiple measurements are recorded. The system samples the microphone signals at a frequency of 50000 Hz over a period of 0.2 s. Afterwards the system needs 0.4 s to package the data and send it to the host computer. These two steps are repeated over the whole measurement time. This means that at the end of a measurement, a number of data-blocks are obtained. Since the experiment is considered to be a statistically stationary process, all the blocks can be averaged to reduce noise [5]. A measurement contains approximately 25 blocks and the result of the averaging is clearly visible in the spectral analysis of the microphone signals.

Horizontal scaling

For most of the test cases in these experiments, the sound sources are expected uniformly over the whole span of the airfoil edges, or the rod. However due to irregularities, like a circular cross-section of the wind tunnel, this is not always shown by a source plot. The beamforming algorithm tends to only detect and show the most intense spot in the field of view. In order to correct for this effect all the pixel lines perpendicular to the span of the airfoil can be scaled separately. This will make sure that along the span, all sources are equally powerful, so a uniform spanwise source distribution is obtained. This method is inspired by techniques described in [6] and [7]. This however makes the scale on the source plot obsolete. This horizontal scaling is only useful for sound source identification, not for determining the exact intensity. The effect of this process is illustrated by Fig. 5 and 6. Both figures are produced from the same dataset. In this case the rod is parallel to the airfoil's leading edge and had a diameter of 4 mm. The wind speed is 30 m/s and the frequency range is 1550 to 1620 Hz.

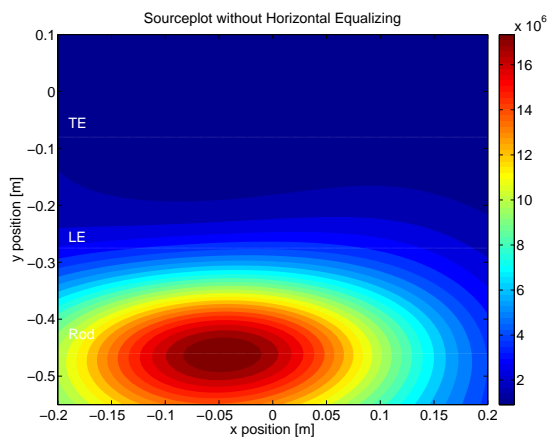


Figure 5: Without horizontal scaling

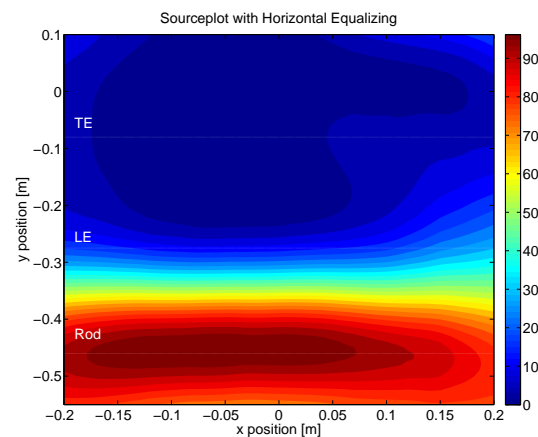


Figure 6: With horizontal scaling

3 Results and discussion

In this section the results of the measurement campaign will be presented and discussed. The results are divided among the three test cases described in section 2. Below each figure the represented test case will be given with there corresponding letter as depicted in Fig. 1. Furthermore the freestream velocity V_∞ , the rod diameter d_r and the frequency range f will be given below each figure. The colour scales used in the figures show the relative normalised power emitted at the shown source locations, as perceived at the receiver's location. In all the presented cases the wind corrected steering vector described in section 2.2 was used. In almost all cases the loudest source in the test was the rod placed in the flow. The focus of this paper is how the shed vorticity reacts on the airfoil. Therefore the source plots created use frequency ranges outside the frequency range produced by the rod (given by the Strouhal relation). The frequency ranges of interest are determined based on the spectral analysis of a data set. The lowest wind speed used in the experiment sequence is 25 m s^{-1} , since at lower wind speeds the

frequency of the shed vorticity becomes too low to result in useful resolutions. In each picture every pixel represents 2 x 2 mm of the scanned region, this determines the finest difference that can be mapped in a source plot. This is not a limitation, but was chosen for convenience. This pixel size results in reasonable computing time and is sufficient for these experiments. In total 48 measurements were recorded, however to avoid repetition only the most interesting results will be shown and discussed.

3.1 One rod parallel

This section treats case (a) shown in Fig. 1, where one rod is placed upstream, parallel to the airfoil. Since in this case noise is expected to be uniform along the span of the wing, horizontal scaling is applied in all figures in this section. From Fig. 7, 9, 11, 12 and 13 it is clear that for this test case, the noise emitted at the leading edge can clearly be identified. This confirms the expectation that the rod causes vortex shedding which causes noise when it impinges on the airfoil leading edge. The noise emitted from the leading edge is nearly continuous over the entire span of the airfoil. This confirms that the horizontal scaling as introduced in section 2.2, gives appropriate results. Furthermore the noise is located at a line which nearly coincides with the leading edge of the airfoil, confirming that the wind scaling is done correctly. For the case where the rod with a 3 mm cross-section is used, it is also possible to identify the noise emitted at the trailing edge, as illustrated in Fig. 8 and 10. In contrast, when the 4 mm diameter rod was used, the noise at the trailing edge of the airfoil was non-identifiable. This could be due to the fact that the frequency of the noise emitted by the rod coincides with the noise emitted at the trailing edge.

When focussing on the frequencies of the source plots a number of relations can be derived. The first two follow directly from the Strouhal relation, namely that a higher velocity leads to higher frequencies and that a thicker rod leads to lower frequencies. Next to this it can be noted that the frequency of the sound detected at the leading edge is always lower than the predicted frequency of vortex shedding by the rod, when using the Strouhal with a Strouhal number of 0.21. For example in Fig. 7 the Strouhal relation predicts a frequency of 2100Hz, whereas the frequency where the noise emitted at the leading edge is found ranges from 1500Hz to 1400Hz. When only focussing on the test case with a rod diameter of 3 mm, it can also be noted that the noise emitted at the trailing edge has a higher frequency than the noise emitted at the leading edge.

3.2 One rod perpendicular

This section treats case b in Fig. 1, where one rod is placed upstream, perpendicular to the rod. Since for this test set-up it is not expected to have uniform noise sources across the span, horizontal scaling is not applied here. A first observation in Fig 14 to 18 is that the presence of the rod is most easily distinguished at the trailing edge of the airfoil and not on the leading edge. This might be due to the fact that the vorticity shed behind the perpendicular rod is restricted to a finite part of the airfoil's span. The resulting surface pressure perturbations are scattered from the trailing edge. A second observation is that the highest noise emission is located at an x-position of approximately 7 cm to the right of the centre of the phased array. This corresponds

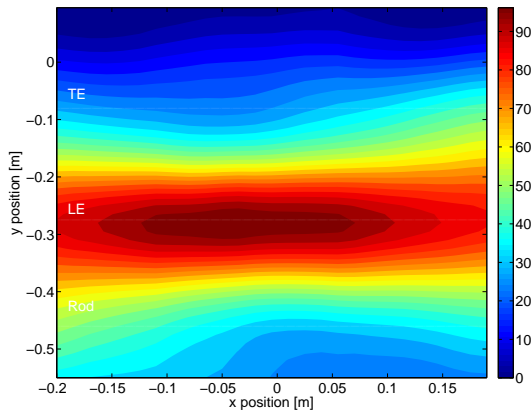


Figure 7: case a
 $V_\infty = 30 \text{ ms}^{-1}$
 $1300 \text{ Hz} < f < 1400 \text{ Hz}$
 $d_{r1} = 3 \text{ mm}$

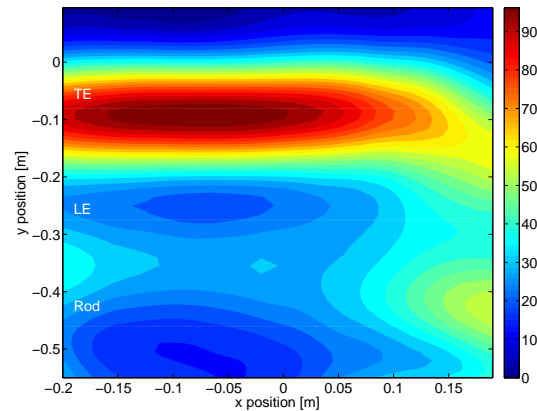


Figure 8: case a
 $V_\infty = 30 \text{ ms}^{-1}$
 $1700 \text{ Hz} < f < 1800 \text{ Hz}$
 $d_{r1} = 3 \text{ mm}$

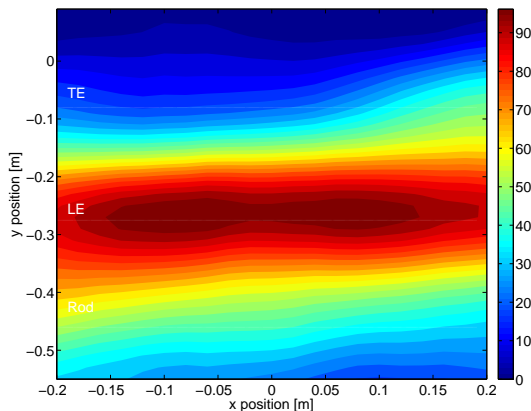


Figure 9: case a
 $V_\infty = 35 \text{ ms}^{-1}$
 $1400 \text{ Hz} < f < 1500 \text{ Hz}$
 $d_{r1} = 3 \text{ mm}$

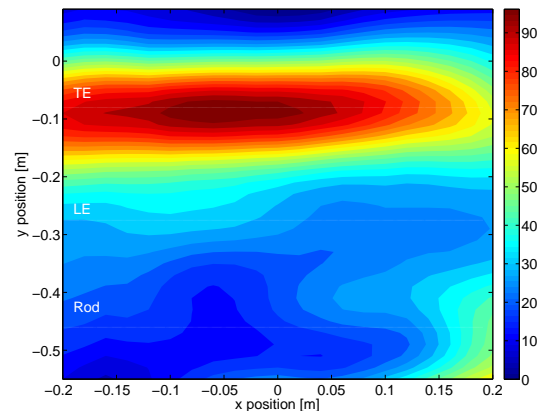


Figure 10: case a
 $V_\infty = 35 \text{ ms}^{-1}$
 $1900 \text{ Hz} < f < 2000 \text{ Hz}$
 $d_{r1} = 3 \text{ mm}$

to our test-up since the rod was placed in the middle of the wind tunnel and the centre of the phased array was positioned 7 cm to the left of the centre line of the wind tunnel. Furthermore it can be noted that for the case where the rod with a diameter of 3 mm was used, the source plots are not as clear. This could be caused by the fact that also the trailing edge of the airfoil has a thickness of 3 mm. When comparing the frequency range of the trailing edge noise of the perpendicular rod case (Fig. 8) to the parallel rod case (Fig. 15) with the same parameters, it is clear that the perpendicular rod-airfoil test set-up leads to higher frequencies.

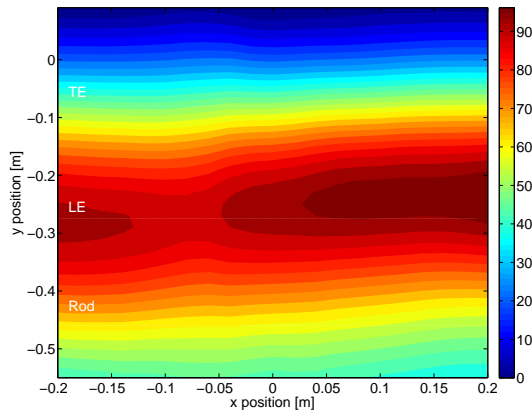


Figure 11: case a
 $V_\infty = 25 \text{ ms}^{-1}$
 $1000 \text{ Hz} < f < 1100 \text{ Hz}$
 $d_{r1} = 4 \text{ mm}$

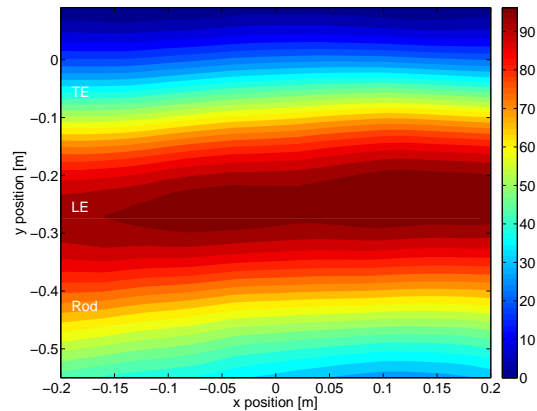


Figure 12: case a
 $V_\infty = 30 \text{ ms}^{-1}$
 $1100 \text{ Hz} < f < 1200 \text{ Hz}$
 $d_{r1} = 4 \text{ mm}$

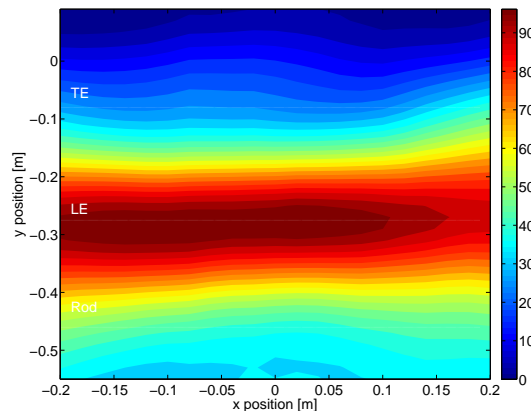


Figure 13: case a
 $V_\infty = 35 \text{ ms}^{-1}$
 $1300 \text{ Hz} < f < 1400 \text{ Hz}$
 $d_{r1} = 4 \text{ mm}$

3.3 Two rods perpendicular

This section shows the results for test case c (Fig. 1), where two rods were placed at a distance of 14cm apart and perpendicular to the airfoil. The main conclusion that can be drawn is that the source plot maps the position of the two rods at an accuracy of approximately 1cm. This confirms that the phased array has a high enough accuracy to be useful in a wind tunnel environment for noise source identification. Moreover it should be noted that the noise can be identified at both the level of the rod itself and at the trailing edge of the airfoil. However,

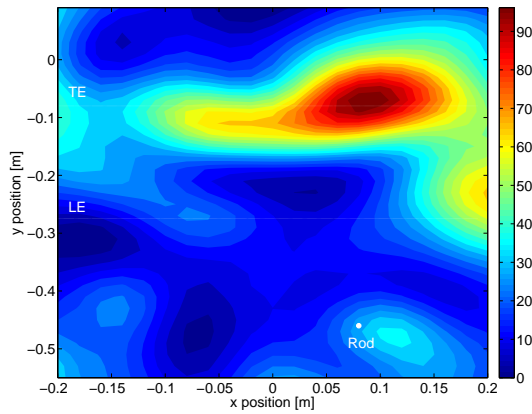


Figure 14: case b
 $V_\infty = 25 \text{ ms}^{-1}$
 $2450 \text{ Hz} < f < 2550 \text{ Hz}$
 $d_{r1} = 3 \text{ mm}$

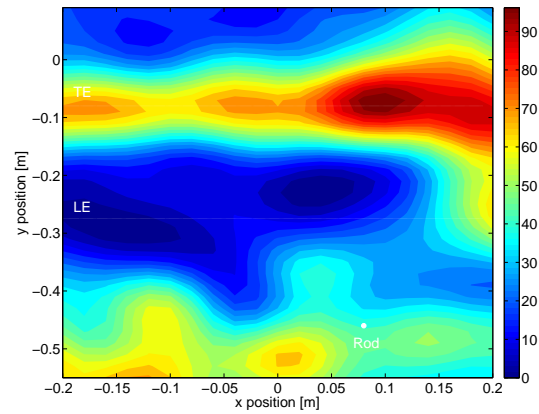


Figure 15: case b
 $V_\infty = 30 \text{ ms}^{-1}$
 $2550 \text{ Hz} < f < 2650 \text{ Hz}$
 $d_{r1} = 3 \text{ mm}$

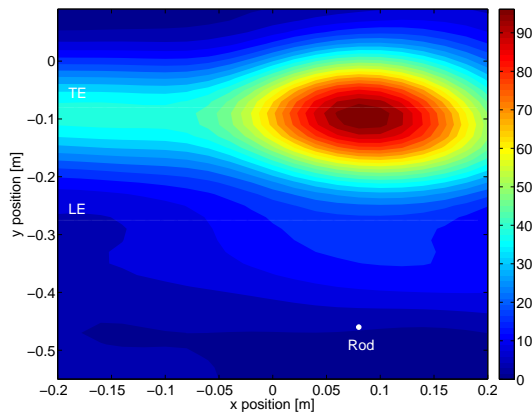


Figure 16: case b
 $V_\infty = 25 \text{ ms}^{-1}$
 $1700 \text{ Hz} < f < 1800 \text{ Hz}$
 $d_{r1} = 4 \text{ mm}$

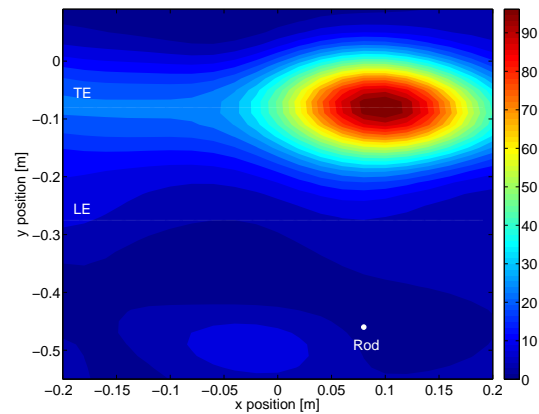


Figure 17: case b
 $V_\infty = 30 \text{ ms}^{-1}$
 $2050 \text{ Hz} < f < 2150 \text{ Hz}$
 $d_{r1} = 4 \text{ mm}$

similar to case b, at the leading of the airfoil no noise emission is found. This would mean that in the case of a rod placed upstream perpendicular to an airfoil the noise scattered at the trailing edge is of higher intensity than the noise cause by the shed vorticity impinging on the leading edge.

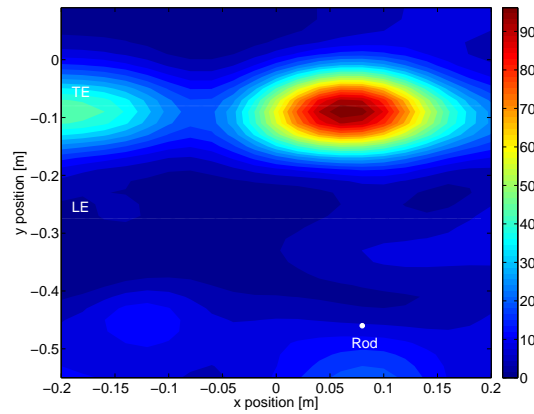


Figure 18: case b
 $V_\infty = 35 \text{ ms}^{-1}$
 $2350 \text{ Hz} < f < 2450 \text{ Hz}$
 $d_{r1} = 4 \text{ mm}$

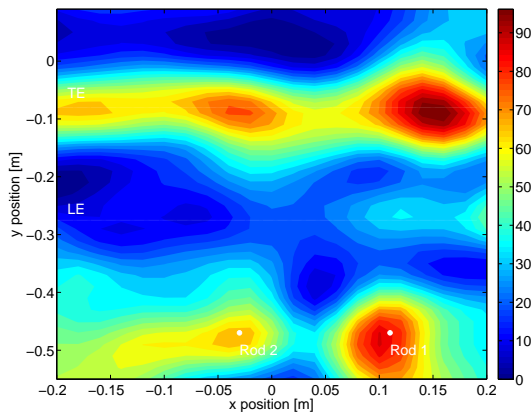


Figure 19: case c
 $V_\infty = 35 \text{ ms}^{-1}$
 $2850 \text{ Hz} < f < 2950 \text{ Hz}$
 $d_{r1} = 3 \text{ mm}$
 $d_{r2} = 4 \text{ mm}$

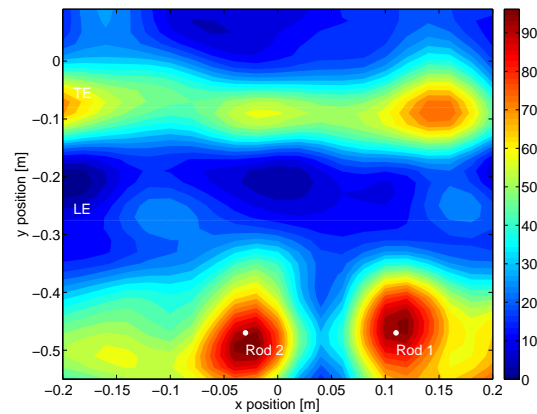


Figure 20: case c
 $V_\infty = 40 \text{ ms}^{-1}$
 $2600 \text{ Hz} < f < 2800 \text{ Hz}$
 $d_{r1} = 3 \text{ mm}$
 $d_{r2} = 4 \text{ mm}$

4 Conclusion

The purpose of this research is to determine if the developed low cost acoustic camera is suitable for wind tunnel measurements. To prepare the camera for wind tunnel measurements, three adaptations are done to the beamforming algorithm:

- Wind-correction to obtain a higher precision

- Averaging to filter out noise from the environment
- Horizontal scaling to identify noise over the whole airfoil span width

With these corrections measurements are performed in an open-jet non-anechoic vertical wind tunnel at flow speeds ranging from 15 m s^{-1} to 40 m s^{-1} . The model used in the wind tunnel is a generic symmetric airfoil in combination with one or two rods placed upstream the airfoil. The results in section 3 show that different noise emitters in the wind tunnel set-up can clearly be separated which validates the implemented adaptations and the usefulness of this camera in a wind tunnel environment.

References

- [1] R. P. Dougherty. “Beamforming in Acoustic Testing.” In *Aeroacoustic Measurements* (edited by T. J. Mueller), chapter 2, pages 62–97. Springer-Verlag Berlin Heidelberg New York, 2002. ISBN 3-540-41757-5.
- [2] M. C. Jacob, J. Boudet, D. Casalino, and M. Michard. “A rod-airfoil experiment as a benchmark for broadband noise modeling.” *Theoretical and Computational Fluid Dynamics*, 19(3), 171–196, 2005. URL <http://www.springerlink.com/index/M1E9PXKD9ERT9PMC.pdf>.
- [3] V. Lorenzoni. “Aeroacoustic investigation of rod-airfoil noise based on time-resolved piv.” Master of science thesis, Delft University of Technology, Delft, Netherlands, 2008. URL http://www.lr.tudelft.nl/fileadmin/Faculteit/LR/Organisatie/Afdelingen_en_Leerstoelen/Afdeling_AEWE/Aerodynamics/Contributor_Area/Secretary/M._Sc._theses/doc/081227_thesis_Valerio_Lorenzoni.pdf.
- [4] S. Oerlemans and P. Sijtsma. “Acoustic array measurements of a 1:10.6 scaled airbus a340 model.” *AIAA Paper*, (2004-2924), 2004. URL <http://www.springerlink.com/index/M1E9PXKD9ERT9PMC.pdf>.
- [5] S. Oerlemans and P. Sijtsma. “Phased array beamforming applied to wind tunnel and fly-over tests.” Technical report, National Aerospace Laboratory, 2010.
- [6] P. Sijtsma. “Acoustic array measurements of a 1:10.6 scaled airbus a340 model.” Technical report, National Aerospace Laboratory, 2004.
- [7] P. Sijtsma. “Acoustic array measurements at nlr.”, 2010. Presentation.
- [8] R. van der Goot, M. Boon, J. Hendriks, K. Scheper, G. Hermans, W. van der Wal, D. Ragni, and D. Simons. “A Low Cost, High Resolution Acoustic Camera with a Flexible Microphone Configuration.” Paper, Delft University of Technology, Delft, Netherlands, 2012.